Immunology
The Journal of cells, molecules, systems and technologies

British Society for immunology

IMMUNOLOGY ORIGINAL ARTICLE

Wiskott–Aldrich syndrome protein controls antigen-presenting cell-driven CD4$^+$ T-cell motility by regulating adhesion to intercellular adhesion molecule-1

Fanny Lafouresse,[1,2,3] Vinicius Cotta-de-Almeida,[4] Gema Malet-Engra,[1,2,3] Anne Galy,[5] Salvatore Valitutti[1,2,3] and Loïc Dupré[1,2,3]

[1]*INSERM, U1043,* [2]*Université Toulouse III Paul-Sabatier, Centre de Physiopathologie de Toulouse Purpan,* [3]*CNRS, U5282, Toulouse, France,* [4]*Instituto Oswaldo Cruz, FIOCRUZ, Rio de Janeiro, Brazil and* [5]*INSERM, U951, Généthon, Evry, France*

doi:10.1111/j.1365-2567.2012.03620.x
Received 17 February 2012; revised 21 June 2012; accepted 28 June 2012.
Correspondence: Loïc Dupré, INSERM U1043, Purpan University Hospital, 31300 Toulouse, France.
Email: loic.dupre@inserm.fr
Senior author: Loïc Dupré

Summary

T-cell scanning for antigen-presenting cells (APC) is a finely tuned process. Whereas non-cognate APC trigger T-cell motility via chemokines and intercellular adhesion molecule-1 (ICAM-1), cognate APC deliver a stop signal resulting from antigen recognition. We tested *in vitro* the contribution of the actin cytoskeleton regulator Wiskott–Aldrich syndrome protein (WASP) to the scanning activity of primary human CD4$^+$ T cells. WASP knock-down resulted in increased T-cell motility upon encounter with non-cognate dendritic cells or B cells and reduced capacity to stop following antigen recognition. The high motility of WASP-deficient T cells was accompanied by a diminished ability to round up and to stabilize pauses. WASP-deficient T cells migrated in a normal proportion towards CXCL12, CCL19 and CCL21, but displayed an increased adhesion and elongation on ICAM-1. The elongated morphology of WASP-deficient T cells was related to a reduced confinement of high-affinity lymphocyte function-associated antigen 1 to the mid-cell zone. Our data therefore indicate that WASP controls CD4$^+$ T-cell motility upon APC encounter by regulating lymphocyte function-associated antigen 1 spatial distribution.

Keywords: antigen-presenting cell scanning; lymphocyte function-associated antigen 1; T-cell motility; Wiskott–Aldrich syndrome protein.

Introduction

Efficacious and controlled adaptive immune responses depend on fine tuning of the motility behaviour of T cells, during their search for antigen-presenting cells (APC) in lymphoid organs and peripheral tissues.[1] Intravital microscopy analysis has revealed that, in the absence of antigen, T cells crawl in an amoeboid manner within lymph nodes, cycling between highly motile and non-motile states.[2] In the presence of antigen, the recognition of cognate APC by the engagement of the T-cell receptor delivers a stop signal through lymphocyte-function-associated antigen 1 (LFA-1) -driven adhesion strengthening.[3] This allows sustained T-cell/APC interactions to take place[4] in the form of immunological synapses that will orchestrate the antigenic activation.[5,6] Although T-cell motility during scanning may appear as a random behaviour, it is controlled by adhesive and chemotactic signals provided by both cellular and extracellular components of the tissue environment.[7] In addition to the fibroblastic reticular cell network that guides T-cell trajectories,[8] APC themselves are key regulators of T-cell motility. Indeed, non-cognate APC trigger T-cell motility, a step required for efficient exploration of cognate APC.[9] Moreover, non-cognate dendritic cells (DC) presenting self-antigen deliver homeostatic signals to CD4$^+$ T cells that promote survival and increase responsiveness to subsequent encounters with cognate APC.[10–12] The DC-driven CD4$^+$ T-cell motility can be recapitulated *in vitro* with speed and motility behaviour comparable to those observed in lymph nodes.[4,13] Experiments *in vitro* have shown that intercellular adhesion molecule 1 (ICAM-1) and chemo-

Abbreviations: shRNA short hairpin RNA; WAS Wiskott–Aldrich syndrome; WASP Wiskott–Aldrich syndrome protein; iDC immature dendritic cells

kines produced by immature DC (iDC) are responsible for the induction of T-cell motility.[13]

Although the motility signals delivered by APC contribute to setting the pulse to $CD4^+$ T-cell scanning, it remains to be investigated which molecules integrate these signals from the T-cell side. Actin cytoskeleton remodelling proteins are known to be of central importance for the control of T-cell motility in response to chemokines and in complex tissue environments.[14] A regulator of actin cytoskeleton in haematopoietic cells is the Wiskott–Aldrich syndrome protein (WASP), which deficiency causes the Wiskott–Aldrich syndrome (WAS). A combination of defects affecting T-cell activation is believed to contribute to the abnormal immune responses accounting for the high susceptibility of WAS patients to develop infections, malignancies and autoimmune disorders. In the context of WAS, T-cell encounter with APC may be reduced or delayed because WASP has been reported to regulate T-cell chemotaxis[15] and homing to secondary lymphoid organs.[16,17] Furthermore, upon encounter with cognate APC, WASP appears to tune T-cell activation by regulating immunological synapse assembly through local actin polymerization.[18–20] Recent studies based on live imaging have further defined the role of WASP as a molecule promoting symmetry and focused T-cell receptor engagement at the immunological synapse.[21,22]

Given the evidence of a functional contribution of WASP to T-cell migration and immunological synapse dynamics, we investigated whether WASP could regulate T-cell scanning. In particular, we focused on the phase of T-cell motility driven by non-cognate APC. Primary human $CD4^+$ T cells in which WASP was knocked-down with a short hairpin RNA (shRNA) -encoding lentiviral vector elongated abnormally and displayed a reduced propensity to pause at the contact with autologous iDC. The abnormal scanning behaviour of WASP-deficient T cells was linked to a spatial dispersion of high-affinity LFA-1. Our study therefore unravels a new role of WASP as a brake that controls T-cell motility during APC scanning.

Materials and methods

Cell lines

Blood samples from patients with WAS and healthy donors were obtained following standard ethical procedures and as per French Bioethics law and with the approval of the local ethics committee. Patients WAS_1 and WAS_2 were reported by Calvez *et al.*[22] and are known to have defective WASP expression. Patient WAS_4 was reported by Trifari *et al.*[23] and is known to express WASP in half of his $CD4^+$ T cells as a result of spontaneous corrective mutation. $CD4^+$ T cells were directly isolated from the blood of healthy donors by negative depletion using Rosette Sep (StemCell Technologies, Vancouver, BC, Canada). $V\beta_2^+$ $CD4^+$ T cells were then positively selected by incubating the $CD4^+$ T cells with a phycoerythrin (PE) -labelled anti-T-cell receptor $V\beta_2$ monoclonal antibody (mAb; Beckman Coulter, Fullerton, CA) followed by magnetic sorting (StemCell Technologies). Freshly isolated $V\beta_2^+$ $CD4^+$ T cells were expanded with anti-CD3/CD28-coated Dynabeads (Invitrogen, Carlsbad, CA) in RPMI-1640 containing 5% human serum and 100 U/ml interleukin-2. The $V\beta_2^+$ $CD4^+$ T cell lines were restimulated as described above every 19–21 days. $V\beta_2^+$ $CD4^+$ T cells from a WAS patient and a control healthy donor were generated as previously described.[22] The $V\beta_2^+$ $CD4^+$ T cells were used for functional assays when they had regained a resting state (14–21 days after activation). Epstein–Barr virus-transformed B cells (JY cell line) were cultured in complete medium (RPMI-1640 containing 10% fetal calf serum). $CD14^+$ cells were obtained by positive magnetic cell purification (Miltenyi Biotec, Bergisch Gladbach, Germany) and differentiated into iDC by a 6-day culture in complete medium supplemented with interleukin-4 and granulocyte–macrophage colony-stimulating factor (R&D Systems, Minneapolis, MN). The phenotype of the different cell types was assessed by FACS analysis (FACSCalibur; BD Biosciences, San Jose, CA) using PE-labelled anti-TCR$V\beta_2$ mAb (Beckman Coulter), PE-CY5-labelled anti-CD4 mAb, FITC-labelled anti-CD14 mAb, PE-Cy5-labelled anti-CD11c mAb, FITC-labelled anti-HLA-DR, DP, DQ mAb, PE-labelled anti-CD83 mAb and FITC-labelled anti-CD86 mAb (all from BD Biosciences). Results were analysed with the FlowJo software (Tree Star, Ashland, OR). Purity of $V\beta_2^+$ $CD4^+$ T cells and iDC was routinely between 95 and 99%.

Transduction with shRNA-encoding lentiviral vectors

At day 3 after stimulation with anti-CD3/CD28-coated beads, $V\beta_2^+$ $CD4^+$ T cells were transduced with previously optimized lentiviral vectors encoding green fluorescent protein (GFP) and two copies of the shRNA sequences targeting WAS or an irrelevant control (scramble).[24] Transduction was performed at a multiplicity of infection of 30 over 6 h in RPMI-1640 containing 5% human serum, interleukin-2 (100 U/ml) and polybrene (4 μg/ml). At day 10 after transduction, GFP-positive $CD4^+$ T cells were sorted on a FACSAria II sorter (BD Biosciences). Transduced cells were analysed for GFP and WASP expression by FACS. Cells were fixed/permeabilized, labelled with anti-WASP mAb (5A5; BD Biosciences) followed by A647-labelled GAM-IgG2a mAb (Invitrogen) and subsequently acquired on a FACSCalibur cytometer and analysed using the FlowJo software. The inhibition of WASP expression was

assessed in parallel by Western blot, as previously described.[22] Proliferation of transduced T cells was measured by liquid scintillation counting of [^{3}H]thymidine incorporation following stimulation for 72 hr with immobilized anti-CD3 mAb (OKT3; ebiosciences, San Diego, CA).

Expression analysis of chemokines, chemokine receptors and ICAM-1/LFA-1

The JY cells and iDC were fixed with 1% paraformaldehyde, then stained with anti-CXCL12 mAb (K15C, kindly provided by F. Arenzana-Seisdedos) or an anti-CCL19 mAb (R&D systems) followed by A488-labelled GAM IgG2a or A488-labelled GAM IgG2b mAb, respectively (Invitrogen) or with PE-labelled anti-ICAM-1 Ab (BD Biosciences). $CD4^+$ T cells were incubated with PE-labelled anti-CXCR4 antibody or with an A647-labelled anti-CCR7 antibody (both from BD Pharmingen, San Jose, CA). Expression of LFA-1 conformation was measured by a 5-min incubation with the following antibodies: HI111 (Biolegend, San Diego, CA), KIM127 (kindly provided by N. Hogg), 24 (Abcam, Cambridge, UK), then incubated for an additional 5 min with 1 μg/ml CXCL12 (Peprotech, London, UK), washed and incubated with A647-labelled anti-IGg1 mAb (Invitrogen). All samples were subsequently acquired on a FASCScan or FACSCalibur cytometer (BD Biosciences) and analysed using the FlowJo software.

Survival assay

$V\beta_2^+$ $CD4^+$ T cells (1×10^5) were cultured alone or in the presence of iDC ($0{\cdot}5 \times 10^5$) in serum-free medium. After 2, 4 and 6 days of culture, cells were harvested and stained with 7-AAD (BD Biosciences). Expression of 7-AAD was subsequently measured on a FACSCalibur cytometer (BD Biosciences) and analysed with the FlowJo software. Cell survival was determined as the percentage of 7-AAD-positive T cells over total T cells.

Transwell assay

Migration assays were performed in 24-chamber plates using Transwell inserts with 5-μm pores (Costar, Cambridge, MA). $V\beta_2^+$ $CD4^+$ T cells (5×10^5) were placed onto the upper chamber in serum-free medium while the lower chamber was filled with serum-free medium supplemented or not with CXCL12, CCL19 or CCL21 (Peprotech) at the indicated concentration. After 2 hr of incubation at 37° in 5% CO_2, cells that migrated into the lower chamber were harvested and counted with reference beads (Calibration beads; BD Biosciences) on a FACSCalibur cytometer (BD Biosciences). The percentage of migrating cells was determined as follows: number of migrating cells (lower chamber)/total number of cells (input) $\times$ 100. To measure JY cell-driven $V\beta_2^+$ $CD4^+$ T-cell transmigration, PFA-fixed JY cells loaded or not with TSST-1 superantigen (Toxin Technology, Sarasota, FL) were incubated for 8 min with T cells at the JY : T-cell ratio indicated and then transferred onto the upper chamber of a Transwell. Following 3-hr incubation at 37° in 5% CO_2, the percentage of transmigrating T cells was determined as above.

Video microscopy

$V\beta_2^+$ $CD4^+$ T cells ($0{\cdot}2 \times 10^5$) and APC ($0{\cdot}1 \times 10^5$) were incubated for 8 min and transferred to poly-D-lysine-coated Lab-Tek chambers (Nunc, Rochester, NY). Under some conditions, T cells were pre-treated overnight with pertussis toxin (Calbiochem, Darmstadt, Germany) or for 1 hr with anti-LFA-1 blocking antibody (HI111). Cells were recorded at 37° in 5% CO_2 on an LSM 510 confocal microscope equipped with a $\times$ 40–1·3 oil immersion Plan-Apochromat objective (CarlZeiss AG, Jena, Germany). Using the multi-position macro of the Zeiss LSM Image Browser, the different cell types were recorded in parallel for 2 hr. For each film, 20 cells were tracked with the Manual Tracking plugin of the ImageJ software (U.S National Institutes of Health, Bethesda, MD). Tracks were plotted by fixing the starting location of each cell at the *x-y* graph origin using the Chemotaxis Tools of Ibidi (Martinsried, Germany). Motility parameters, including mean velocity, accumulated distance, maximal distance from origin, instantaneous velocity, pause frequency and pause duration were calculated using Ibidi chemotaxis tools and a macro developed by D. Sapède (INSERM). For the measurement of adhesion to ICAM-1, $CD4^+$ T cells were incubated for 10 min on Lab-Tek chambers coated with recombinant ICAM-1/Fc chimera (10 μg/ml; R&D Systems). Cells were recorded over 5 min at 37° in 5% CO_2 on an LSM 510 confocal microscope equipped with a $\times$ 40–1·3 oil immersion Plan-Apochromat objective. Adhesion was calculated as the fraction of cells adhering to the coated surface in relation to the total number of cells. Adherent cells were identified by the emission of various protrusions over the ICAM-1-coated surface, whereas non-adherent cells were identified as inert cells floating above the bottom of the chambers. The roundness coefficient of the cells was measured after 10-min incubation on ICAM-1 by drawing the outline of each cell using the LiveWire 2D plugin of ImageJ and applying the Roundness Coefficient of ImageJ.

Immunofluorescence staining

To investigate the spatial distribution of LFA-1 under its intermediate-affinity and high-affinity conformations, $V\beta_2^+$ $CD4^+$ T cells were seeded for 30 min at 37° onto

glass slides (Erie Scientific, Portsmouth, NH) coated with 10 μg/ml recombinant ICAM-1/Fc chimera, then fixed with 3% paraformaldehyde and permeabilized with 0·1% saponin and 3% BSA. Cells were stained with anti-WASP antibody (H-250; Santa Cruz Biotechnology, Santa Cruz, CA) and with either KIM127 or 24 antibody, followed by A647-labelled anti-rabbit antibody and A546-labelled anti-IgG1 antibody (both from Invitrogen). F-actin was stained with A350-labelled phalloidin (Molecular Probes, Eugene, OR). Slides were mounted with in 90% glycerol-PBS containing 2·5% 1,4-diazabicyclo[2.2.2]octane (Fluka, Geneva, Switzerland) and examined with an LSM 710 confocal microscope equipped with a × 63–1·4 oil immersion Plan-Apochromat objective (CarlZeiss AG). The profile of 24 and KIM-127 antibody staining intensity was measured on ImageJ by tracing a line along the longitudinal T-cell axis, from the leading edge to the tip of the uropod. To compare the distribution of the high-affinity and intermediate-affinity LFA-1 in WASP-positive and WASP-depleted cells, the area under the curve for the 24 antibody staining was calculated at the mid-body (10–14 μm) and the area under the curve for the KIM127 antibody staining was calculated at the cell front (1–3 μm) and at the cell rear (12–22 μm). To investigate local actin polarization and cell morphology, Vβ_2^+ CD4$^+$ T cells were incubated with latex beads pre-coated with 10 μg/ml recombinant ICAM-1/Fc chimera at a 2 : 1 cell to bead ratio for 30 min. Cell–bead conjugates were seeded on poly-D-lysine-coated glass slides, then fixed with 3% paraformaldehyde and permeabilized with 0·1% saponin and 3% BSA. Cells were stained with anti-WASP antibody (H-250; Santa Cruz Biotechnology) followed by A633-labelled anti-rabbit antibody (Invitrogen) and with A546-labelled phalloidin (Molecular Probes). Slides were mounted with 90% glycerol-PBS containing 2·5% 1,4-diazabicyclo[2·2·2]octane and examined with an LSM 710 confocal microscope equipped with a × 63–1·4 oil immersion Plan-Apochromat objective (CarlZeiss AG).

Results

Generation of WASP-deficient primary human CD4$^+$ T cells

To investigate the role of WASP in the scanning behaviour of human CD4$^+$ T cells, its expression was knocked-down in Vβ2$^+$ CD4$^+$ T cells purified from the blood of healthy donors. For that purpose, CD4$^+$ T cells were transduced with a lentiviral vector encoding two copies of a WASP-specific shRNA (shWASP) and expressing GFP as a reporter gene, allowing purification of transduced cells by flow cell sorting. WASP expression was efficiently inhibited in transduced cells as shown by flow cytometry and confirmed by Western blot analysis (Fig. 1a,b). In comparison, the transduction of primary human CD4$^+$ T cells with a control vector encoding a control scramble shRNA and GFP (shControl) had no effect on WASP expression. In shWASP CD4$^+$ T cells, WASP expression remained at undetectable levels following several stimulation cycles, indicating that a stable inhibition of WASP expression was achieved (data not shown). The shRNA-mediated WASP knock-down approach was then validated at a functional level because shWASP CD4$^+$ T cells harboured a proliferation defect following TCR stimulation (Fig. 1c), as previously described for CD4$^+$ T cells from WAS patients.[22] Therefore, primary human CD4$^+$ T cells transduced with the shWASP lentiviral vector can be used as a relevant model to study the role of WASP in T-cell scanning.

Increased motility of WASP-deficient CD4$^+$ T cells upon contact with non-cognate APC

To first investigate the role of WASP in non-cognate APC-induced T-cell motility, live CD4$^+$ T cells and fixed Epstein–Barr virus-transformed B cells (JY cell line) were seeded in the upper chamber of a Transwell. T-cell motility was assessed as the capacity of T cells to transmigrate to the lower Transwell chamber within 3 hr. In the absence of JY cells, approximately 10% of control and WASP-deficient CD4$^+$ T cells were able to transmigrate (Fig. 2a). In the presence of JY cells, the transmigration of control CD4$^+$ T cells was increased, thereby revealing JY cell-induced T-cell motility. Reproducibly, the JY cell-induced motility of shWASP T cells was higher than that of control T cells (+ 41% on average). The increased motility of WASP-deficient T cells was confirmed when titrating down the number of JY cells and thereby reducing the JY : T ratio (see Supplementary material, Fig. S1a). Given the increased motility of WASP-deficient CD4$^+$ T cells upon encounter with non-cognate JY cells, we next assessed their capacity to stop upon encounter with JY cells presenting increasing concentrations of TSST-1 superantigen (Fig. 2b). At high superantigen doses (1 and 10 ng/ml), the JY cell-induced transmigration of both shControl and shWASP CD4$^+$ T cells was prevented, indicating that WASP deficiency did not alter the sensing of the superantigen-driven stop signal. Nevertheless, shWASP CD4$^+$ T cells remained more mobile than shControl cells in the presence of JY cells presenting a lower dose of TSST-1 (0·1 ng/ml). To investigate the functional consequence of the increased motility of shWASP CD4$^+$ T cells, cell survival promoted by APC was measured over 6 days of culture (Fig. 2c). In the absence of APC, the mortality rate of shWASP CD4$^+$ T cells was slightly increased compared with shControl CD4$^+$ T cells. As expected, the presence of APC (iDC) strongly diminished the mortality of shControl CD4$^+$ T cells. Interestingly, iDC reduced spontaneous death of shWASP CD4$^+$ T cells to a level comparable to that of

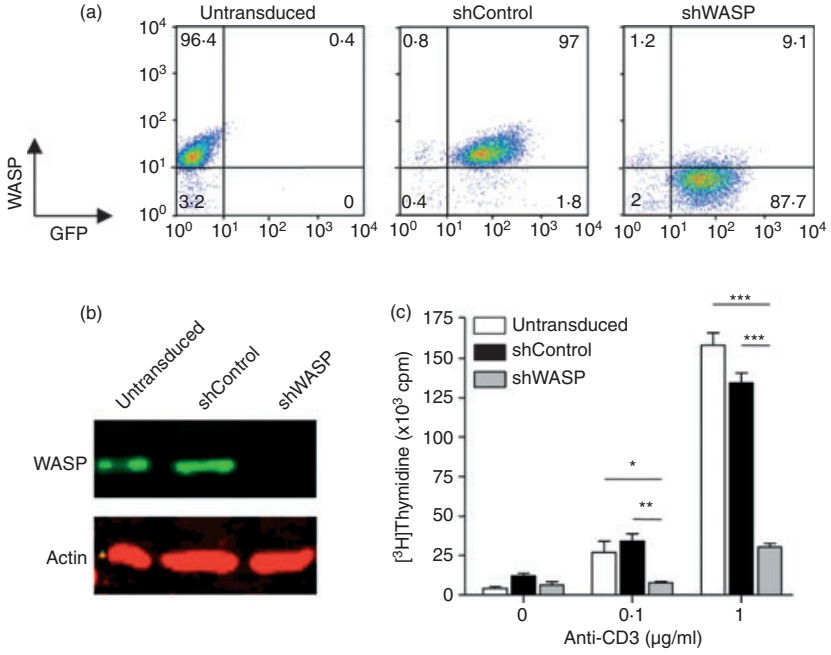

Figure 1. Short hairpin (sh) RNA-mediated Wiskott–Aldrich syndrome protein (WASP) knock-down in primary human CD4$^+$ T cells. Representative example of CD4$^+$ T cells transduced with lentiviral vectors encoding green fluorescent protein (GFP) and either shControl or shWASP. (a) Untransduced and GFP-sorted shControl and shWASP CD4$^+$ T cells were analysed for GFP and WASP expression by flow cytometry. (b) Untransduced and GFP-sorted shControl and shWASP CD4$^+$ T cells were analysed for WASP expression by Western blot. (c) Anti-CD3-induced proliferation of untransduced and GFP-sorted shControl and shWASP CD4$^+$ T cells was measured by [^{3}H]thymidine incorporation. Data correspond to the mean ± SEM of three replicates. *$P < 0{\cdot}05$; **$P < 0{\cdot}01$; ***$P < 0{\cdot}001$ unpaired t test.

shControl CD4$^+$ T cells. Collectively, these data reveal that the abnormally high APC-driven T-cell motility observed in WASP-deficient T cells may counteract their capacity to stop following antigen recognition and neutralize their increased spontaneous death.

WASP-deficient CD4$^+$ T cells pause less upon contact with non-cognate APC

To better characterize the high motility behaviour of WASP-deficient CD4$^+$ T cells in the presence of non-cognate APC, we tracked shControl and shWASP CD4$^+$ T cells by real-time microscopy as they encountered autologous iDC (Fig. 3a) or JY cells (see Supplementary material, Fig. S1b). In the presence of non-cognate APC, CD4$^+$ T cells acquired a random motile behaviour as illustrated by their multidirectional migratory paths. Notably, the proportion of fast-migrating CD4$^+$ T cells (> 1·8 μm/min, red tracks) was higher for shWASP CD4$^+$ T cells than for shControl CD4$^+$ T cells. WASP-deficient T cells were very motile within a confined area relatively close to their starting position (Fig. 3a and Supplementary material, Fig. S1b). Accordingly, the analysis of APC-induced motility parameters (Fig. 3b and Supplementary material, Fig. S1c) showed that, compared with shControl CD4$^+$ T cells, shWASP CD4$^+$ T cells acquired a higher mean velocity and an increased accumulated distance, without moving further away from their origin. We then investigated whether the increased motility of shWASP CD4$^+$ T cells was related to a higher instantaneous speed. The speed of both shControl and shWASP CD4$^+$ T cells fluctuated over time within a comparable range of 0 – 25 μm/min. However, when considering the alternation of motile phases (white areas) and pauses (grey areas), shWASP CD4$^+$ T cells spent less time in pause than control cells over the observation period (Figs. 3c and Supplementary material, Fig. S2a). This was linked to a decreased pause length rather than to a reduced pause frequency (see Supplementary material, Fig. S2b). Together, these data show that in the context of non-cognate iDC encounter, WASP-deficient T cells harbour a restless scanning behaviour because of a reduced ability to pause.

WASP-deficiency promotes CD4$^+$ T-cell adhesion to ICAM-1

T-cell motility induced by non-cognate APC has been shown to depend on both chemokines and ICAM-1 present at the APC surface.[13] Using pertussis toxin, we first confirmed in our model that signalling through chemokine receptors was contributing to APC-induced T-cell motility (Fig. 4a). Blocking the stimulation through chemokine receptors affected APC-induced motility of

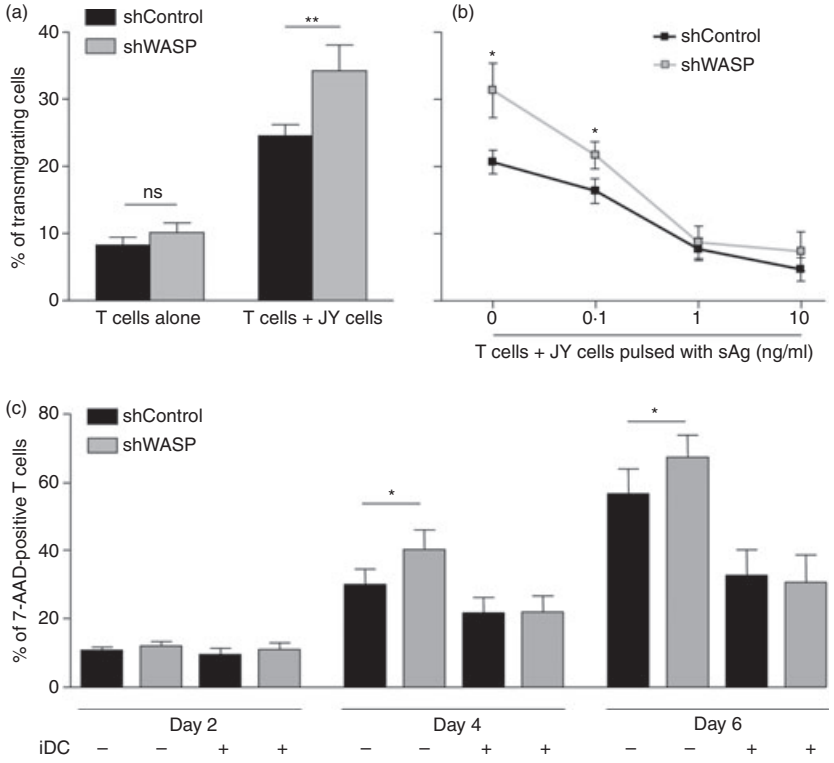

Figure 2. Wiskott–Aldrich syndrome protein (WASP) -deficient $CD4^+$ T cells are hyper-motile at the contact with JY cells. (a) short hairpin (sh) Control or shWASP $CD4^+$ T cells were seeded in the upper chamber of a Transwell with or without fixed JY cells in the absence of antigen at a 1 : 2 JY cell to T-cell ratio. Percentage of transmigrating cells was calculated as the fraction of $CD4^+$ T cells that migrated to the lower chambers, filled with serum-free medium, within 3 hr. The figure represents the mean ± SEM of 13 independent experiments performed with a total of six donors. (b) The shControl or shWASP $CD4^+$ T cells were incubated with fixed JY cells pulsed with increasing concentrations of TSST-1 superantigen. Percentage of transmigrating cells was calculated as in (a). Data correspond to the mean ± SEM of three independent experiments performed with two donors. (c) Either shControl or shWASP $CD4^+$ T cells were cultured in serum-free medium over 6 days with or without immature dendritic cells. T-cell mortality was assessed by measuring 7-AAD-positive cells. Data correspond to the mean ± SEM of five independent experiments performed with four donors. $*P < 0{\cdot}05$; $**P < 0{\cdot}01$ paired *t* test.

WASP-deficient T cells, indicating that the increased motility of these cells may be driven by an abnormal response to chemokines. We investigated in our model whether the main chemokines recognized by $CD4^+$ T cells were present at the surface of APC. Whereas CCL19 was bound at the surface of both iDC and JY cells, CXCL12 was detected only at the surface of iDC (Fig. 4b). The basal expression of the corresponding chemokine receptors CXCR4 and CCR7 was not altered in shWASP $CD4^+$ T cells compared with shControl $CD4^+$ T cells (Fig. 4c). Moreover, WASP deficiency did not interfere with CXCR4 internalization following CXCL12 stimulation (data not shown). Using a Transwell assay, we unexpectedly observed that shWASP $CD4^+$ T cells migrated toward CXCL12, in a dose–response manner, as efficiently as shControl and untransduced $CD4^+$ T cells (Fig. 4d). The shWASP $CD4^+$ T cells also migrated normally toward CCL19 and CCL21 (Fig. 4d). To confirm that WASP deficiency did not alter human $CD4^+$ T-cell migration toward chemokines *in vitro*, the chemotactic responses of $CD4^+$ T cells isolated from patients with WAS and from healthy donors were compared. The WAS $CD4^+$ T cells expressed normal levels of CXCR4 and CCR7 (see Supplementary material, Fig. S3a) and were able to migrate toward CXCL12, CCL19 and CCL21, as efficiently as control $CD4^+$ T cells (see Supplementary material, Fig. S3b, c). Among the patients studied here, WAS_4 patient had the particularity of being able to express WASP in approximately half of his $CD4^+$ T cells as the result of a spontaneous corrective mutation in the WAS gene (see Supplementary material, Fig. S3d). The proportion of WASP-positive and WASP-negative $CD4^+$ T cells from WAS_4 patient was preserved in those cells that had migrated toward CXCL12 at the two concentrations tested. This reveals that neither WASP-positive nor WASP-negative $CD4^+$ T cells had a chemotactic advantage in this assay. Together, these results clearly demonstrate that in primary human $CD4^+$ T cells, WASP

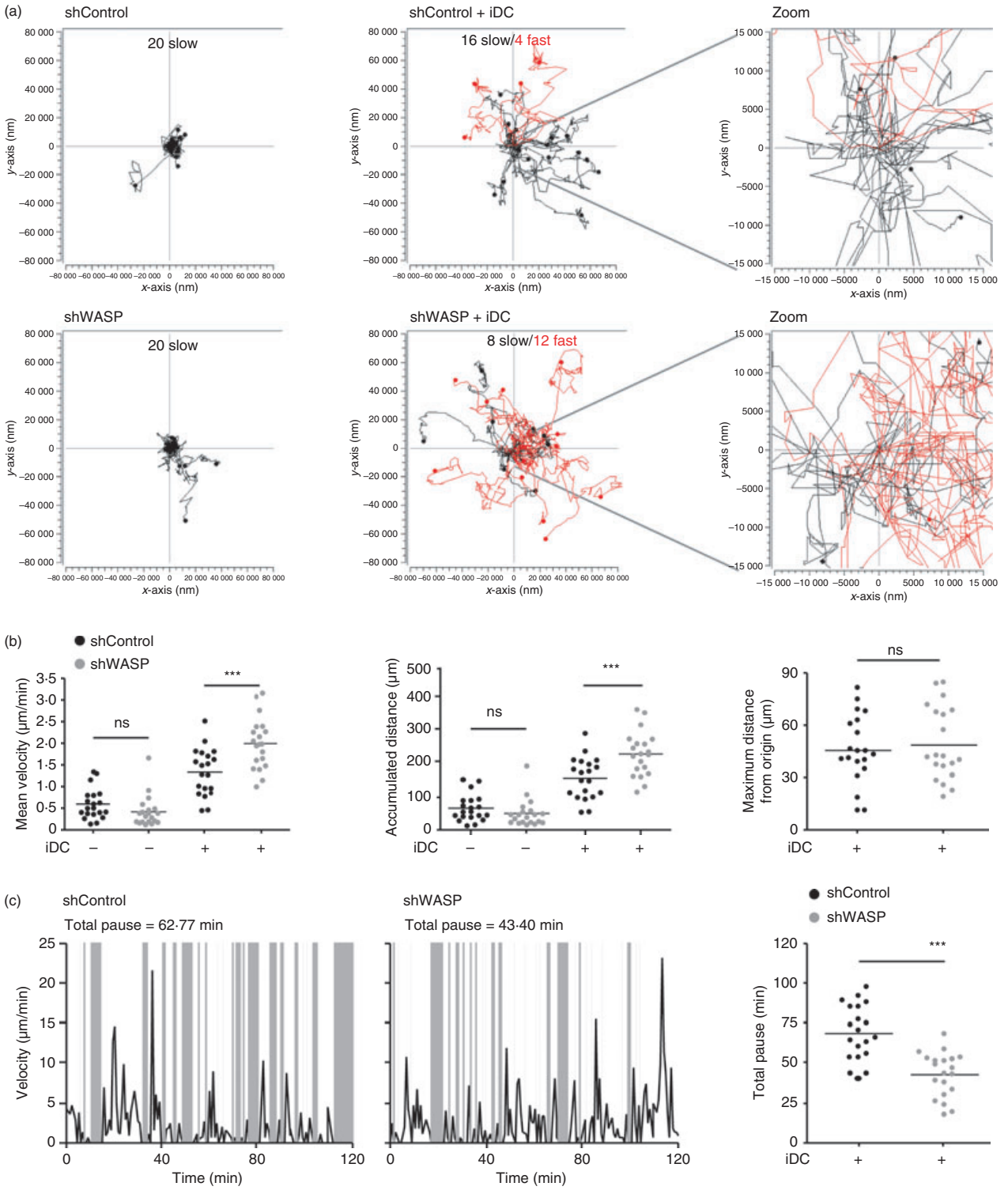

Figure 3. Upon contact with non-cognate immature dendritic cells (iDC), Wiskott–Aldrich syndrome protein (WASP) -deficient $CD4^+$ T cells adopt a hyper-motile behaviour with reduced pause. Short hairpin (sh) Control and shWASP $CD4^+$ T cells alone or with autologous iDC were recorded during 120 min with a time lapse of 46·5 seconds. (a) Motility tracks of 20 individual T cells and corresponding zooms centred around the starting location. Tracks of fast (mean velocity > 1·8 μm/min) and slow (mean velocity < 1·8 μm/min) migrating T cells are shown in red and black, respectively. (b) Mean velocity, accumulated distance and maximum distance from origin of 20 individual shControl and shWASP T cells are shown. (c) Fluctuation of instantaneous velocity over 120 min of one representative shControl T cell and one representative shWASP T cell. Corresponding analysis of total time spent in pause over 120 min of 20 individual shControl and shWASP T cells. Data are from one representative experiment out of four experiments performed with two donors. ***$P < 0{\cdot}001$ unpaired t test.

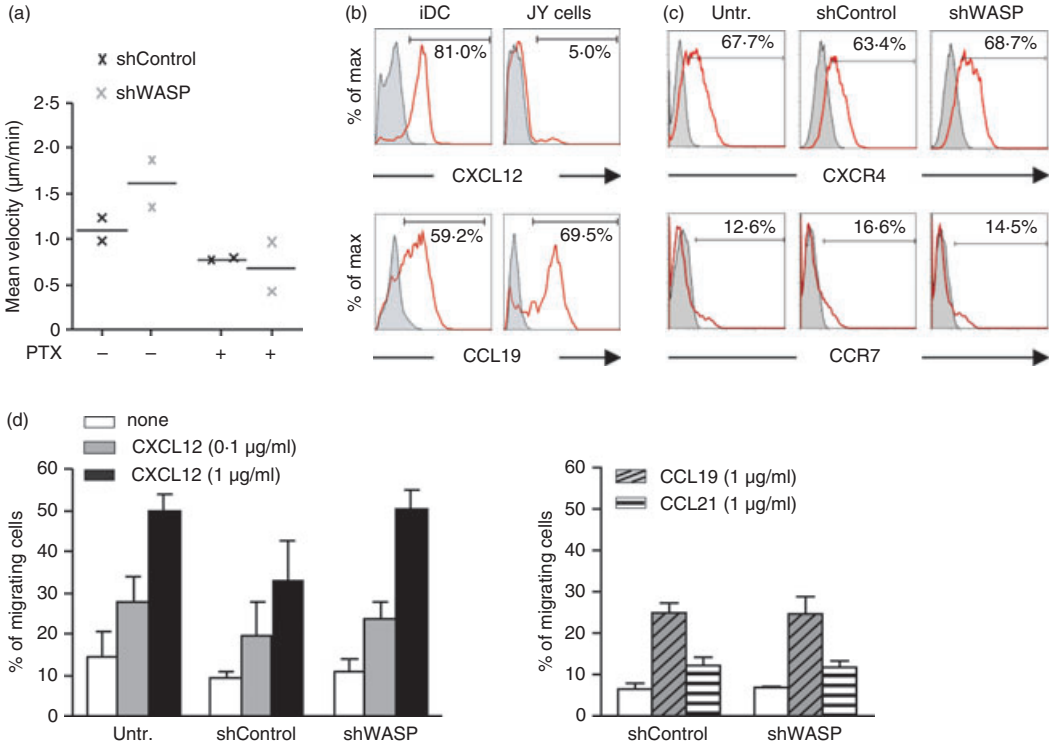

Figure 4. Wiskott–Aldrich syndrome protein (WASP) -deficient $CD4^+$ T cells migrate in a normal proportion toward CXCL12, CCL19 and CCL21. (a) Short hairpin (sh) Control and shWASP $CD4^+$ T cells treated or not with pertussis toxin were video recorded, during 120 min with a time lapse of 46·5 seconds, upon contact with JY cells and the mean velocity of 20 individual T cells was measured. Results show the mean of two experiments performed with two donors. (b) CXCL12 and CCL19 expression on immature dendritic cells (iDC) and JY cells. Staining with corresponding isotype controls is shown in grey. (c) CXCR4 and CCR7 expression on untransduced, shControl and shWASP $CD4^+$ T cells. Staining with corresponding isotype controls is shown in grey. (d) Untransduced, shControl or shWASP $CD4^+$ T cells were seeded in the upper chamber of a Transwell, and the percentage of migrating cells was calculated as the fraction of $CD4^+$ T cells that migrated to the lower chamber, filled with the indicated chemokine, within 2 hr. Data correspond to the mean ± SEM of three independent experiments performed with three donors. No statistical difference was revealed by paired *t*-test.

is dispensable for *in vitro* migration toward CXCL12, CCL19 and CCL21.

We then examined whether WASP may rather be involved in adhesion to ICAM-1 in our model. Using anti-LFA-1 blocking antibody, we confirmed that signalling through LFA-1 was also contributing to APC-induced T-cell motility (Fig. 5a). Blocking the stimulation through LFA-1 inhibited the increased APC-induced motility of WASP-deficient T cells, indicating that this dysfunction may be induced by an abnormal response to ICAM-1. As expected, ICAM-1 was present at the surface of both iDC and JY cells (Fig. 5b). Total LFA-1 as well as LFA-1 under intermediate-affinity and high-affinity conformation was expressed at comparable levels in shWASP and shControl $CD4^+$ T cells (Fig. 5c,d). Furthermore, intermediate-affinity and high-affinity LFA-1 levels increased similarly in shWASP and shControl $CD4^+$ T cells upon CXCL12 stimulation. Clearly however, a higher percentage of WASP-deficient $CD4^+$ T cells adhered on ICAM-1-coated slides compared with control cells (Fig. 5e). These results show that in the absence of WASP, $CD4^+$ T cells were more prone to adhere on ICAM-1, even if they expressed normal levels of LFA-1 under its different conformations. This implies that the abnormally high APC-driven motility of WASP-deficient T cells may be related to an abnormal adhesion to ICAM-1, rather than to an abnormal chemotactic ability.

Increased ICAM-1-driven elongation in WASP-deficient T cells

How to reconcile the increased ICAM-1 adhesion with the enhanced motility observed in WASP-deficient T cells? To answer this question, we first analysed the morphology of these cells upon ICAM-1 stimulation. The proportion of WASP-deficient T cells that elongated on ICAM-1-coated slides was increased compared with control cells (Fig. 6a). This was further illustrated by the measurement of cell roundness showing that in the

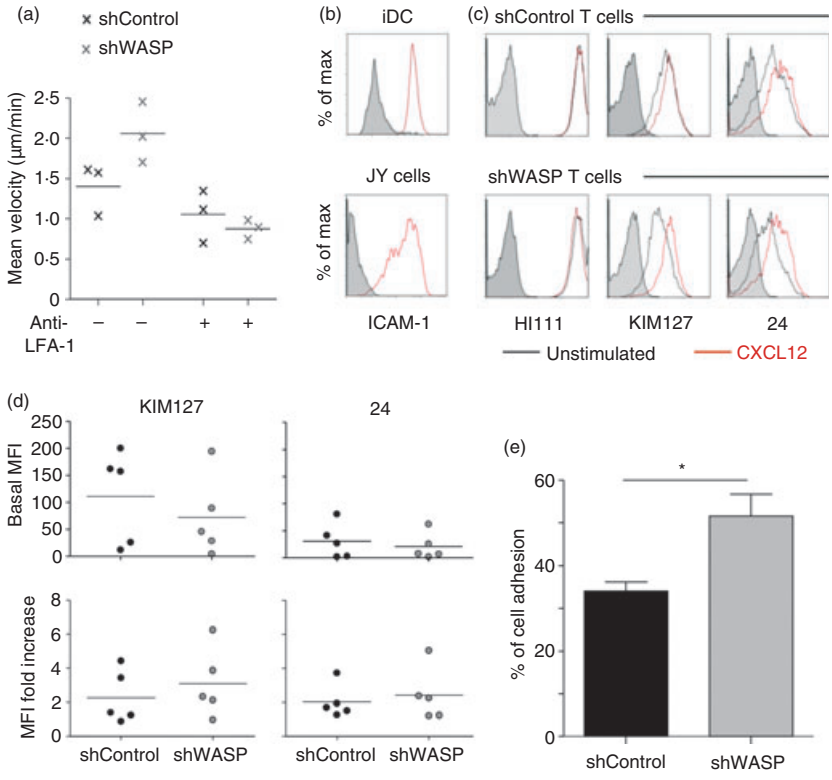

Figure 5. Wiskott–Aldrich syndrome protein (WASP) -deficient $CD4^+$ T cells display an increased adhesion on intercellular adhesion molecule 1 (ICAM-1). (a) Short hairpin (sh) Control and shWASP $CD4^+$ T cells treated or not with blocking anti-lymphocyte function-associated antigen 1 (LFA-1) antibody were video recorded, during 120 min with a time lapse of 46·5 seconds, upon contact with JY cells and the mean velocity of 20 individual T cells was measured. Results show the mean of three experiments performed with three donors. (b) ICAM-1 expression on immature dendritic cells (iDC) and JY cells. Staining with corresponding isotype control is shown in grey. (c) LFA-1 expression under its total (HI111), intermediate-affinity (KIM127) and high-affinity (24) conformations on shControl and shWASP $CD4^+$ T cells either unstimulated or stimulated with CXCL12. Staining with corresponding isotype controls is shown in grey. (d) KIM127 and 24 basal geometric mean fluorescence intensity (MFI) values and MFI fold increase upon CXCL12 stimulation of three independent experiments performed with five donors are shown. No statistical difference was revealed by paired *t*-test. (e) Percentage of adhesive shControl and shWASP $CD4^+$ T cells on ICAM-1-coated slides. Data correspond to the mean ± SEM of four independent experiments performed with three donors. A total number of 265 shControl and 265 shWASP $CD4^+$ T cells were counted. $^*P < 0{\cdot}05$ Mann–Whitney *U*-test.

absence of WASP the fraction of round cells diminished. $CD4^+$ T cells were then incubated with ICAM-1-coated latex beads, to investigate F-actin polymerization at the site of ICAM-1 stimulation. As shown in Fig. 6(b), most of the control T cells establishing contacts with beads remained relatively spherical (morphology 'type 1'). In accordance with the data above, a higher percentage of WASP-deficient T cells elongated upon contact with ICAM-1-coated latex beads (morphology 'type 2'). Both shControl and shWASP $CD4^+$ T cells displayed polarized actin cytoskeleton surrounding the beads. However, in contrast to control cells, a substantial proportion of WASP-deficient $CD4^+$ T cells establishing contacts with beads protruded actin-rich structures away from the bead-contact sites (morphology 'type 3'). Finally, we used real-time microscopy to study morphology dynamics of shControl and shWASP $CD4^+$ T cells upon encounter with non-cognate iDC (Fig. 6c and Supplementary material, Videos S1 and S2). In agreement with their elongation on ICAM-1, WASP-deficient $CD4^+$ T cells coming into contact with iDC stretched extensively. This morphology was associated to motility. Interestingly, actively scanning WASP-deficient $CD4^+$ T cells remained in close contact with APC, occasionally losing contact for a short time when crawling from one APC to another. Indeed, their elongated shape was characterized by a uropod that appeared to stick to iDC (red arrows) and a dynamic leading edge. Compared with control T cells, WASP-deficient T cells in contact with iDC displayed a reduced propensity to round up (white arrows). These results therefore link the increased adhesiveness of WASP-deficient T cells to a higher propensity to elongate and to actively scan an APC-rich environment. Moreover, these data corroborate the notion that the increased propensity

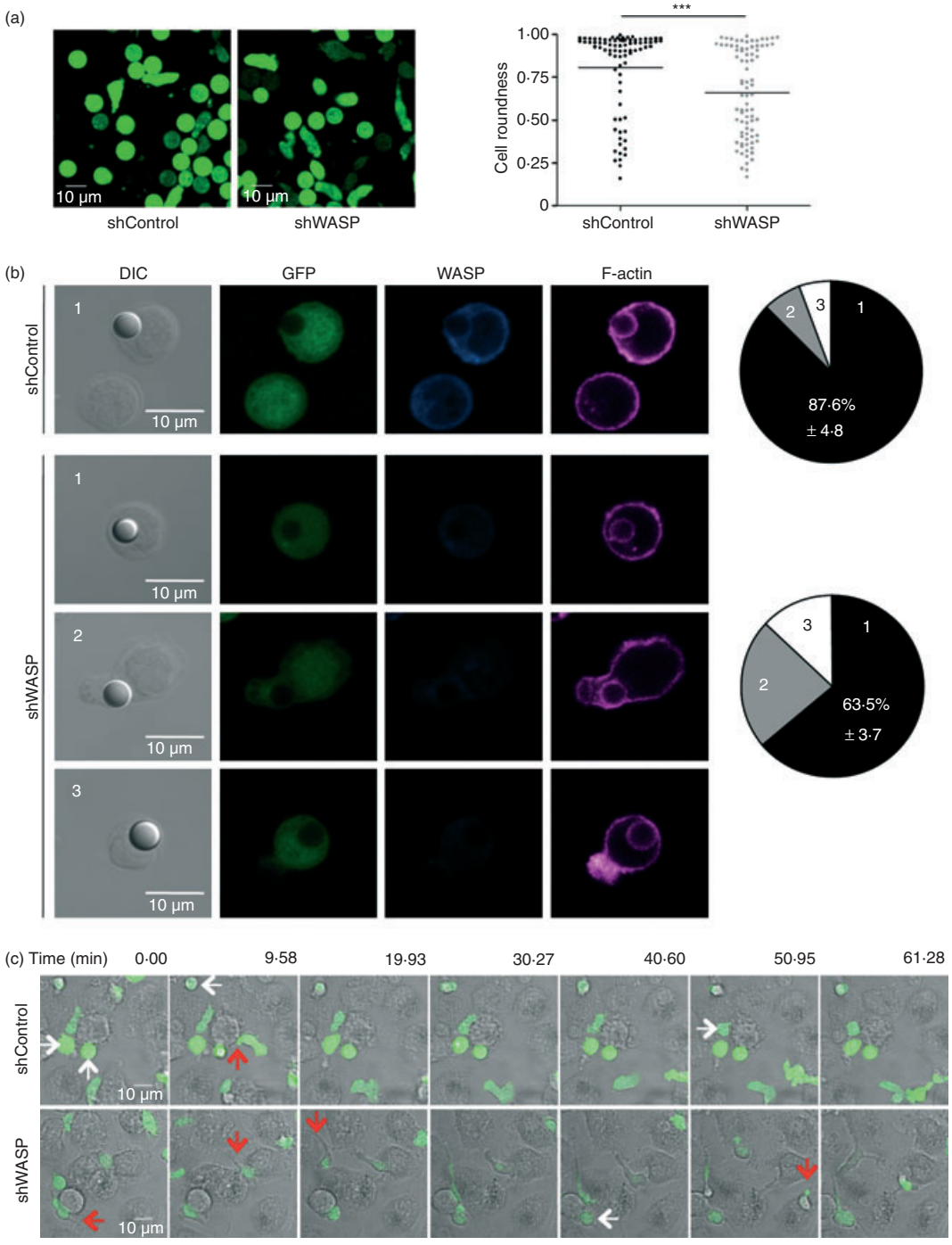

Figure 6. Wiskott–Aldrich syndrome protein (WASP) -deficient $CD4^+$ T cells elongate on intercellular adhesion molecule 1 (ICAM-1) and immature dendritic cells (iDC). (a) Representative images of green fluorescent protein-positive (GFP^+) short hairpin (sh) Control and shWASP $CD4^+$ T cells adhering to ICAM-1. Roundness coefficient of 83 shControl and 83 shWASP $CD4^+$ T cells upon adhesion to ICAM-1. Data are from two independent experiments performed with two donors. ***$P < 0{\cdot}001$ unpaired *t*-test. (b) Representative images of GFP^+ shControl and shWASP $CD4^+$ T cells in conjugation with ICAM-1-coated beads and immunostained for WASP and F-actin. Percentage of T cells displaying three distinct morphological types defined as follows are represented: type 1: spherical cells with polymerized actin surrounding the bead; type 2: elongated cells; type 3: protruded actin-rich structures away from the bead contact site. Data represent mean ± SEM of two experiments performed with three donors. (c) Movie sequences of shControl and shWASP T cells at the contact of iDC; white arrows indicate cells that round up and red arrows indicate adherent uropods. Results are representative of four experiments performed.

of WASP-deficient T cells to elongate is driven by abnormal integration of ICAM-1 stimulation.

Dispersed high-affinity LFA-1 localization in WASP-deficient T cells

The precise localization of LFA-1 under its intermediate-affinity and high-affinity conformations is key to the tuning of T-cell adhesive properties,[25] so the staining with KIM127 and 24 antibodies (revealing intermediate-affinity and high-affinity LFA-1, respectively) was compared in WASP-deficient and control T cells. Both WASP-deficient and control T cells that adhered to ICAM-1 adopted a polarized morphology with a front enriched in F-actin and a uropod at the rear (Fig. 7a). KIM127 staining showed comparable distribution in both cell types with a narrow enrichment at the front and a wide distribution towards the rear (Fig. 7a,b). Staining with 24 in control T cells was concentrated at the mid-body. However, in WASP-deficient T cells the intensity of the 24 staining at the mid-body was significantly diminished. Instead, WASP-deficient T cells displayed an abnormally broad pattern of high-affinity LFA-1 distribution, which extended along the uropod. These data therefore strongly suggest that the increased propensity of WASP-deficient T cells to adhere to ICAM-1 was a consequence of a defect in restricting high-affinity LFA-1 to the mid-cell region. Altogether, our data suggest that the restless scanning behaviour of WASP-deficient $CD4^+$ T cells might be, at least in part, consecutive to an inability to restrict high-affinity LFA-1 and to stabilize arrest phases at the contact with APC.

Discussion

The function of APC is generally viewed through the restricted angle of cognate interactions with T cells. However, most APC/T-cell encounters *in vivo* are non-cognate. Interactions between steady-state iDC and T cells are expected to take place frequently, either in secondary lymphoid organs or in peripheral tissues. In this context, a key function of DC is to activate T-cell motility to promote efficient scanning. The present study provides insight into the molecular mechanisms regulating the motility programme acquired by effector $CD4^+$ T cells upon encounter with iDC and B cells.

Here, we identify the actin cytoskeleton regulator WASP as a key controller of APC-driven T-cell motility. Our study shows that WASP deficiency in primary human $CD4^+$ T cells enhanced APC-induced motility *in vitro*. The cause of the enhanced motility of WASP-deficient $CD4^+$ T cells was directly related to a decreased length of time spent under arrest. In contrast to control $CD4^+$ T cells, WASP-deficient $CD4^+$ T cells did not transiently round up upon APC encounter, a phase of scanning normally associated to speed reduction.[26] Instead, at the contact with APC, WASP-deficient $CD4^+$ T cells displayed an abnormally sustained migrating morphology characterized by an active leading edge and an elongated uropod. It has been shown that DC-mediated T-cell survival is dependent on cell-to-cell contact and that it may be driven by signalling originating from the uropod.[27] It would therefore be interesting to test whether the elongated uropod observed in WASP-deficient T cells contributes to their high propensity to survive at the contact with iDC. In our *in vitro* setting, the enhanced motility and the elongated morphology of WASP-deficient T cells did not permit them to reach further distances and to contact more DC. Indeed, the motility of WASP-deficient T cells was restricted to a confined area and this appeared to be related to the fact that WASP-deficient T cells were sticking to APC through their uropod. In apparent contrast, WASP-deficient T cells transmigrated at an increased rate in our Transwell assay. This might be explained by an enhanced scanning activity leading these cells to contact membrane pores more frequently. Moreover, the elongated morphology of WASP-deficient T cells may have facilitated their transmigration. It remains to be tested how the abnormal morphology and the restless scanning of WASP-deficient T cells, observed here *in vitro*, could impact scanning in dense matrices and in natural tissue environments.

The APC-driven T-cell motility is known to be driven by chemokines and ICAM-1.[13] Both chemotaxis in response to various chemokines[15,16,28,29] and adhesion to ICAM-1[30–32] have been reported, in different cell types, to depend on the presence of WASP. Therefore, how could WASP deficiency exacerbate APC-driven T-cell motility? In agreement with previous studies reporting that WASP is dispensable for murine T-cell chemotaxis *in vitro*,[16,17,33] we clearly show that WASP-deficiency, both in shWASP and WAS patient T cells, does not alter chemotaxis to CXCL12. This finding was reinforced by the direct comparison of the chemotaxis of WASP-positive and WASP-negative $CD4^+$ T cells originating from a revertant patient. The discrepancy with a previous study reporting defective CXCL12-driven chemotaxis in $CD3^+$ T cells from WAS patients[15] may be linked to differences in the nature and the maturation stage of the T cells studied. Furthermore, our data indicate that WASP is dispensable to chemotaxis towards CCL19 and CCL21, although the migratory response towards these chemokines was low, as expected for effector T cells expressing low levels of CCR7.

In contrast to their normal ability to migrate in response to chemokines, WASP-deficient T cells adhered at an abnormally high rate on ICAM-1. This result is in accordance with the increased ability of $CD4^+$ T cells from WAS patients to form conjugates with non-cognate APC.[22] The increased adhesion of WASP-deficient T cells

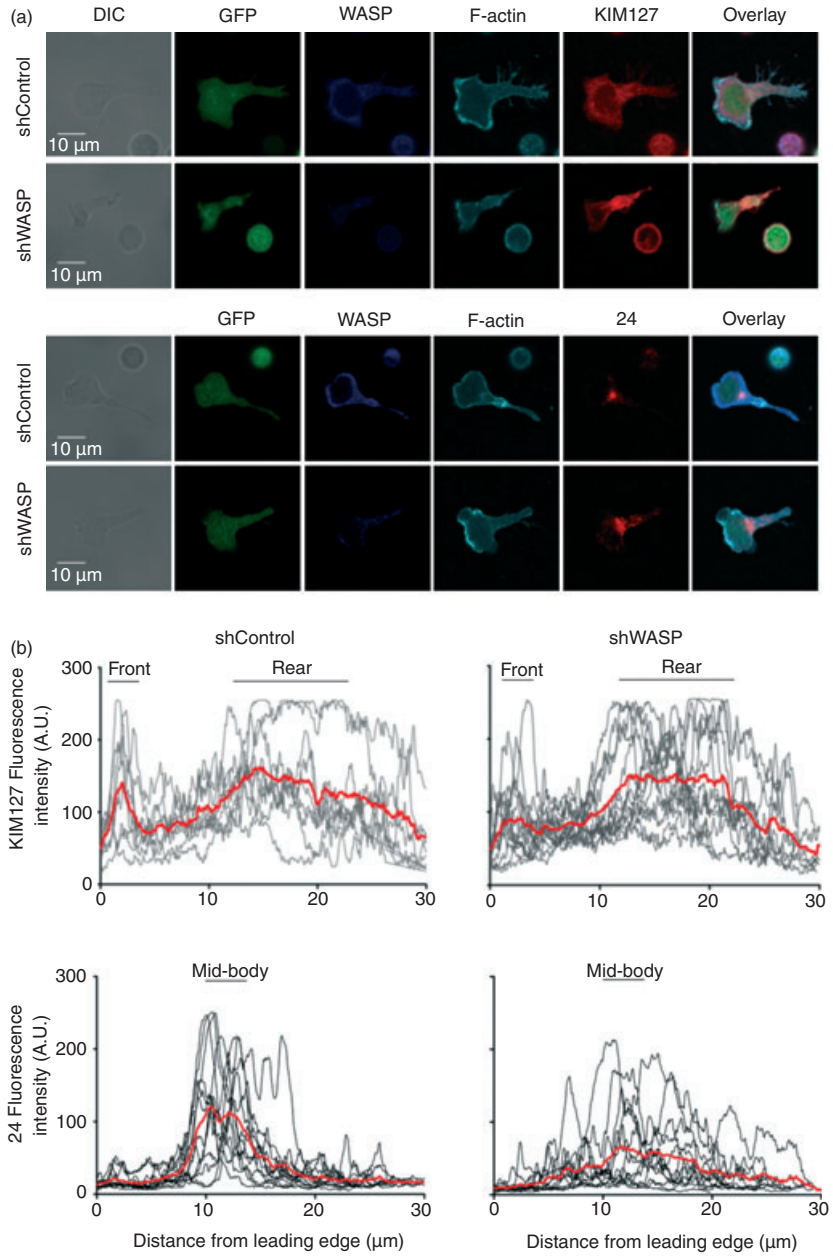

Figure 7. Adhesive Wiskott–Aldrich syndrome protein (WASP) -deficient $CD4^+$ T cells display an abnormal localization of high-affinity lymphocyte function-associated antigen 1 (LFA-1). (a) One representative image of green fluorescent protein-positive (GFP^+) short hairpin (sh) Control and shWASP $CD4^+$ T cells adherent to intercellular adhesion molecule 1 (ICAM-1), immunostained for WASP, F-actin, and KIM127 (upper panel) or 24 (lower panel). (b) KIM127 and 24 monoclonal antibody fluorescence intensity profiles, from the leading edge to the tip of the uropod. Mean fluorescence intensity of 9–13 individual T cells is represented in red. The black bars define the cell regions that were considered for area under the curve calculations. No statistical difference was found between the KIM127 staining of shControl and shWASP $CD4^+$ T cells. The 24 staining at the mid-body was reduced in shWASP $CD4^+$ T cells compared with shControl $CD4^+$ T cells ($P = 0{\cdot}025$ unpaired *t*-test). Data are from one representative experiment out of three experiments performed with three donors.

mirrored an increased proportion of elongated cells that were prompt to move. The exacerbated response of WASP-deficient T cells to ICAM-1 was neither the result of an abnormal expression level of LFA-1 nor of an abnormal conformational activation of LFA-1 following ICAM-1 engagement. However, WASP deficiency resulted in a loose confinement of high-affinity LFA-1 to the mid-cell focal zone and a dispersion towards the uropod. During T-cell scanning of DC surfaces, LFA-1 is dynamically redistributed from the leading edge to the mid-cell zone where it forms a signalling platform.[27] WASP deficiency might therefore affect the spatial organization of LFA-1

signalling. Previous studies have brought to light the concept that the spatial confinement and the dynamics of intermediate-affinity and high-affinity LFA-1 pools are controlled by physical links with the actin cytoskeleton.[25,34] Intermediate-affinity LFA-1 linked to α-actinin-1 permits new adhesions at the leading edge, whereas high-affinity LFA-1 linked to talin provides a central adhesive platform at the mid-cell region. It can be assumed that the widening of the high-affinity LFA-1 spatial distribution in WASP-deficient T cells is the result of a defective anchorage to the actin network. In favour of this hypothesis is the observation in natural killer cells that WASP is recruited by talin to the site of LFA-1 engagement to promote localized actin polymerization.[31] However, in contrast to our data, WASP-deficient natural killer cells fail to adhere to ICAM-1 and fail to polymerize actin at the site of LFA-1 engagement. T cells may therefore have a molecular control of integrin anchorage to the cytoskeleton less strictly dependent on WASP than natural killer cells. The experiments based on the incubation of WASP-deficient T cells with ICAM-1-coated beads show that WASP is dispensable to actin polymerization at the site of LFA-1 engagement, although a mild defect could not be excluded. Interestingly, the contact with ICAM-1-coated beads promoted the formation of actin-rich protrusions away from the contact site, suggesting a decoupling between LFA-1 engagement and actin polymerization. We therefore propose that, in the absence of WASP, both abnormal anchorage of high-affinity LFA-1 to the actin cytoskeleton and LFA-1 signalling into aberrant actin remodelling lead to elongated restless cells.

Our results indicate that during the scanning of APC, WASP favours T-cell stability rather than motility. The role of WASP as a gatekeeper of APC-driven T-cell motility may, at least in part, account for the combination of exacerbated response to self-antigen and defective response to certain pathogens observed in WAS.[35,36] On the one hand, the restless scanning of APC presenting self-antigen might favour the activation of auto-reactive T-cell precursors. Of interest, the morphology of WASP-deficient T cells sticking to iDC via their uropod is reminiscent of the previously described ICAM-1/LFA-1-dependent tethered adhesion on chemokine-bearing APC, a mechanism shown to prepare T cells for antigenic stimulation.[37] The exacerbation of tethered adhesion in the context of WASP deficiency may lead to increased sensitivity to self-antigen. On the other hand, our data indicate that the reduced ability of WASP-deficient T cells to stabilize pauses upon inspection of APC is impacting on their capacity to stop in the context of cognate antigen presentation. An increased threshold for antigen-driven stop in WASP-deficient T cells would reduce the capacity of these cells to respond optimally to low affinity antigen or to antigen present at low concentrations. In conclusion, the present study highlights the fact that APC are endowed with the capacity to activate a WASP-controlled motility programme in effector T cells. It will be interesting to address the contribution of the abnormal T-cell scanning identified here in the physiopathology of WAS, using *in vivo* imaging in WASP knockout mice. Moreover, the murine model would permit the study the role of WASP in the scanning activity of naive T cells. Another open question is whether WASP regulation of T-cell scanning also applies to regulatory T cells because $Foxp3^+$ regulatory T cells are functionally impaired in WAS patients and in WASP-deficient mice.[38–40]

Acknowledgements

We thank Nancy Hogg for providing the anti-LFA-1 KIM127 antibody and Fernando Arenzana-Seisdedos for providing the anti-CXCL12 antibody. We thank Sophie Allard and Daniel Sapède from the IFR150 microscopy platform (Toulouse). We are grateful to Khalil Seye and Véronique Parietti for help with lentiviral vector production and to Zilton Vasconcelos and Maria-Ignes Elsas for help with Transwell experiments and helpful discussions. We also thank Christophe Viret for helpful discussion and Josipa Spoljaric for manuscript editing.

This work was supported by the French National Research Agency (ANR-07-MRAR-022-02 grant 'Physio-WAS' to AG and LD), by the Region Midi-Pyrénées (to LD) and by an INSERM-FIOCRUZ cooperation grant (to FL, LD and VC-A). VC-A is supported by the Brazilian Ministry of Health, CNPq and FAPERJ.

Disclosures

The authors have no financial conflicts of interest.

References

1 Dustin ML. Stop and go traffic to tune T cell responses. *Immunity* 2004; **21**:305–14.
2 Miller MJ, Wei SH, Cahalan MD, Parker I. Autonomous T cell trafficking examined *in vivo* with intravital two-photon microscopy. *Proc Natl Acad Sci U S A* 2003; **100**:2604–9.
3 Dustin ML, Bromley SK, Kan Z, Peterson DA, Unanue ER. Antigen receptor engagement delivers a stop signal to migrating T lymphocytes. *Proc Natl Acad Sci U S A.* 1997; **94**:3909–13.
4 Miller MJ, Hejazi AS, Wei SH, Cahalan MD, Parker I. T cell repertoire scanning is promoted by dynamic dendritic cell behavior and random T cell motility in the lymph node. *Proc Natl Acad Sci U S A.* 2004; **101**:998–1003.
5 Monks CR, Freiberg BA, Kupfer H, Sciaky N, Kupfer A. Three-dimensional segregation of supramolecular activation clusters in T cells. *Nature* 1998; **395**:82–6.
6 Grakoui A, Bromley SK, Sumen C, Davis MM, Shaw AS, Allen PM, Dustin ML. The immunological synapse: a molecular machine controlling T cell activation. *Science* 1999; **285**:221–7.
7 Cahalan MD, Parker I. Choreography of cell motility and interaction dynamics imaged by two-photon microscopy in lymphoid organs. *Annu Rev Immunol* 2008; **26**:585–626.
8 Bajenoff M, Egen JG, Koo LY, Laugier JP, Brau F, Glaichenhaus N, Germain RN. Stromal cell networks regulate lymphocyte entry, migration, and territoriality in lymph nodes. *Immunity* 2006; **25**:989–1001.
9 Fischer UB, Jacovetty EL, Medeiros RB *et al.* MHC class II deprivation impairs CD4 T cell motility and responsiveness to antigen-bearing dendritic cells *in vivo*. *Proc Natl Acad Sci U S A* 2007; **104**:7181–6.

10 Kondo T, Cortese I, Markovic-Plese S, Wandinger KP, Carter C, Brown M, Leitman S, Martin R. Dendritic cells signal T cells in the absence of exogenous antigen. *Nat Immunol* 2001; **2**:932–8.
11 Hochweller K, Wabnitz GH, Samstag Y, Suffner J, Hammerling GJ, Garbi N. Dendritic cells control T cell tonic signaling required for responsiveness to foreign antigen. *Proc Natl Acad Sci U S A* 2010; **107**:5931–6.
12 Revy P, Sospedra M, Barbour B, Trautmann A. Functional antigen-independent synapses formed between T cells and dendritic cells. *Nat Immunol* 2001; **2**:925–31.
13 Real E, Kaiser A, Raposo G, Amara A, Nardin A, Trautmann A, Donnadieu E. Immature dendritic cells (DCs) use chemokines and intercellular adhesion molecule (ICAM)-1, but not DC-specific ICAM-3-grabbing nonintegrin, to stimulate $CD4^+$ T cells in the absence of exogenous antigen. *J Immunol* 2004; **173**:50–60.
14 Samstag Y, Eibert SM, Klemke M, Wabnitz GH. Actin cytoskeletal dynamics in T lymphocyte activation and migration. *J Leukoc Biol* 2003; **73**:30–48.
15 Haddad E, Zugaza JL, Louache F *et al.* The interaction between Cdc42 and WASP is required for SDF-1-induced T-lymphocyte chemotaxis. *Blood* 2001; **97**:33–8.
16 Snapper SB, Meelu P, Nguyen D *et al.* WASP deficiency leads to global defects of directed leukocyte migration *in vitro* and *in vivo*. *J Leukoc Biol* 2005; **77**:993–8.
17 Gallego MD, de laFuente MA, Anton IM, Snapper S, Fuhlbrigge R, Geha RS. WIP and WASP play complementary roles in T cell homing and chemotaxis to SDF-1α. *Int Immunol* 2006; **18**:221–32.
18 Dupre L, Aiuti A, Trifari S, Martino S, Saracco P, Bordignon, C, Roncarolo MG. Wiskott–Aldrich syndrome protein regulates lipid raft dynamics during immunological synapse formation. *Immunity* 2002; **17**:157–66.
19 Badour K, Zhang J, Siminovitch KA. Involvement of the Wiskott–Aldrich syndrome protein and other actin regulatory adaptors in T cell activation. *Semin Immunol* 2004; **16**:395–407.
20 Cannon JL, Burkhardt JK. Differential roles for Wiskott–Aldrich syndrome protein in immune synapse formation and IL-2 production. *J Immunol* 2004; **173**:1658–62.
21 Sims TN, Soos TJ, Xenias HS *et al.* Opposing effects of PKCθ and WASp on symmetry breaking and relocation of the immunological synapse. *Cell* 2007; **129**:773–85.
22 Calvez R, Lafouresse F, De Meester J, Galy A, Valitutti S, Dupre L. The Wiskott–Aldrich syndrome protein permits assembly of a focused immunological synapse enabling sustained T-cell receptor signaling. *Haematologica* 2011; **96**:1415–23.
23 Trifari S, Scaramuzza S, Catucci M *et al.* Revertant T lymphocytes in a patient with Wiskott–Aldrich syndrome: analysis of function and distribution in lymphoid organs. *J Allergy Clin Immunol* 2010; **125**:439–48.
24 Jeanson-Leh L, Blondeau J, Galy A. Optimization of short hairpin RNA for lentiviral-mediated RNAi against WAS. *Biochem Biophys Res Commun* 2007; **362**:498–503.
25 Smith A, Carrasco YR, Stanley P, Kieffer N, Batista FD, Hogg N. A talin-dependent LFA-1 focal zone is formed by rapidly migrating T lymphocytes. *J Cell Biol* 2005; **170**:141–51.
26 Negulescu PA, Krasieva TB, Khan A, Kerschbaum HH, Cahalan MD. Polarity of T cell shape, motility, and sensitivity to antigen. *Immunity* 1996; **4**:421–30.
27 Storim J, Brocker EB, Friedl P. A dynamic immunological synapse mediates homeostatic TCR-dependent and -independent signaling. *Eur J Immunol* 2010; **40**:2741–50.
28 Badolato R, Sozzani S, Malacarne F *et al.* Monocytes from Wiskott–Aldrich patients display reduced chemotaxis and lack of cell polarization in response to monocyte chemoattractant protein-1 and formyl-methionyl-leucyl-phenylalanine. *J Immunol* 1998; **161**:1026–33.
29 Westerberg L, Larsson M, Hardy SJ, Fernandez C, Thrasher AJ, Severinson E. Wiskott–Aldrich syndrome protein deficiency leads to reduced B-cell adhesion, migration, and homing, and a delayed humoral immune response. *Blood* 2005; **105**:1144–52.
30 Zhang H, Schaff UY, Green CE *et al.* Impaired integrin-dependent function in Wiskott –Aldrich syndrome protein-deficient murine and human neutrophils. *Immunity* 2006; **25**:285–95.
31 Mace EM, Zhang J, Siminovitch KA, Takei F. Elucidation of the integrin LFA-1-mediated signaling pathway of actin polarization in natural killer cells. *Blood* 2010; **116**:1272–9.
32 Stabile H, Carlino C, Mazza C *et al.* Impaired NK-cell migration in WAS/XLT patients: role of Cdc42/WASp pathway in the control of chemokine-induced β_2 integrin high-affinity state. *Blood* 2010; **115**:2818–26.
33 Blundell MP, Bouma G, Calle Y, Jones GE, Kinnon C, Thrasher AJ. Improvement of migratory defects in a murine model of Wiskott–Aldrich syndrome gene therapy. *Mol Ther* 2008; **16**:836–44.
34 Stanley P, Smith A, McDowall A, Nicol A, Zicha D, Hogg N. Intermediate-affinity LFA-1 binds α-actinin-1 to control migration at the leading edge of the T cell. *EMBO J* 2008; **27**:62–75.
35 Schurman SH, Candotti F. Autoimmunity in Wiskott–Aldrich syndrome. *Curr Opin Rheumatol* 2003; **15**:446–53.
36 Ochs HD, Thrasher AJ. The Wiskott–Aldrich syndrome. *J Allergy Clin Immunol* 2006; **117**:725–38.
37 Friedman RS, Jacobelli J, Krummel MF. Surface-bound chemokines capture and prime T cells for synapse formation. *Nat Immunol* 2006; **7**:1101–8.
38 Maillard MH, Cotta-de-Almeida V, Takeshima F, Nguyen DD, Michetti P, Nagler C, Bhan AK, Snapper SB. The Wiskott–Aldrich syndrome protein is required for the function of $CD4^+$ $CD25^+$ $Foxp3^+$ regulatory T cells. *J Exp Med* 2007; **204**:381–91.
39 Humblet-Baron S, Sather B, Anover S *et al.* Wiskott–Aldrich syndrome protein is required for regulatory T cell homeostasis. *J Clin Invest* 2007; **117**:407–18.
40 Marangoni F, Trifari S, Scaramuzza S, et al. WASP regulates suppressor activity of human and murine $CD4^+$ $CD25^+$ $FOXP3^+$ natural regulatory T cells. *J Exp Med* 2007; **204**:369–380.

Supporting Information

Additional Supporting Information may be found in the online version of this article:

Figure S1. Wiskott–Aldrich syndrome protein (WASP) -deficient $CD4^+$ T cells are hyper-motile at the contact with JY cells.

Figure S2. Wiskott–Aldrich syndrome protein (WASP) -deficient $CD4^+$ T cells are hyper-motile at the contact with immature dendritic cells.

Figure S3. $CD4^+$ T cells isolated from patients with Wiskott–Aldrich syndrome migrate normally toward CXCL12, CCL19 and CCL21.

Video S1. Scanning of immature DC by control T cells.

Video S2. Scanning of immature DC by Wiskott–Aldrich syndrome protein-deficient T cells.

Please note: Wiley-Blackwell are not responsible for the content or functionality of any supporting materials supplied by the authors. Any queries (other than missing material) should be directed to the corresponding author for the article.